Micro Laser Beam Scanner

ESTEC contract n°4000103902/11/NL/CP

Executive Summary Phase II

1 ESA STUDY CONTRACT REPORT - SPECIMEN

<table>
<tr><td>ESA Contract No

4000103902/11/ NL/CP</td><td colspan="2">SUBJECT

Micro Laser Beam Scanner</td><td>CONTRACTOR

sercalo microtechnology ltd.
EPFL
CSEM
ETHZ</td></tr>
<tr><td>* ESA CR( )No</td><td>* STAR CODE</td><td>No of volumes 1
This is Volume No</td><td>CONTRACTOR'S REFERENCE</td></tr>
<tr><td colspan="4">ABSTRACT:
Phase II of this project consisted of the manufacturing and the environmental testing of 23 laser beam scanners, based on the detailed design of Phase I. Pre-tests like mechanical shock and vibration showed already the robustness of the MEMS scanner. Gamma Radiation and Proton Radiation did not effect the devices. During the tests it turned out, that air damped devices are much more resistant to failure than the oil-immersed devices.

Two sets of driver boards with (100x100) data points of the scan path stored, were successfully used for scan path verification after the environmental tests according to the SOW. The electronics driver boards are populated with non rad hard components, as they were not part of the environmental testing. Never the less, the design rules of the boards includes the ability to easy exchange the electronic components with rad. hard ones.

In the end, two SU passed successfully all environmental tests and the project goal was reached in time.</td></tr>
<tr><td colspan="4">The work described in this report was done under ESA Contract. Responsibility for the contents resides in the author or organization that prepared it.</td></tr>
<tr><td colspan="4">Names of authors:
Cornel Marxer, Peter Herbst, Peter Zweifel, Davor Mance, Antonia Neels , Tobias Bandi, Herbert Shea</td></tr>
<tr><td colspan="2">** NAME OF ESA STUDY MANAGER
Joao do Carmo

DIV: MMO
DIRECTORATE: TEC</td><td colspan="2">** ESA BUDGET HEADING</td></tr>
</table>

2 INTRODUCTION

Rovers travelling on unknown surfaces need optical sensors providing the 2D image and distance information, so called 3D vision systems or 3D imagers. There are active and passive 3D vision systems. The passive 3D vision systems are often stereo cameras (NASA's Mars Explorer). Stereo cameras can provide video rate range images over significant fields of view, but have limited range resolution over large measurement ranges and their performance is dependent on the environment illumination and target contrast. The active 3D vision systems have for instance a laser beam scanning the scene. They use time-of-flight techniques to determine the range and provide the third dimension and are also called imaging LIDARs.
In this activity an important key-component to equip such a 3D vision system, namely the laser scanner, was developed.
The requirements for this activity are driven by the application of rover navigation in future planetary exploration missions like the exo mars project.

Phase I consisted of the design based on specifications and the applications given in the SOW. A numerical model was established and all necessary dimensions, functions and layouts were defined.
In Phase II two main tasks have to be accomplished. First, the manufacturing of a sufficient number of scanner devices that allows two Scanner Units to pass successfully the environmental test program. Task two, the environmental test campaign.

3 SCANNER COMPONENTS

The scanner Unit consists of the following components:
- MEMS chip
- Fiber collimator
- TO8 Package
- MEMS PCB
- Housing with connectors and mounting holes

Based on the design of Phase I a 2D electrostatic driven MEMS mirror with D=1mm, exhibiting very low drift to avoid a feedback loop, was manufactured. Figure 1 depicts the numerical model used in Ansys to simulated the performance under Phase I. On the right picture of Figure 1 a SEM picture of the realized MEMS chip is presented. The proposed MEMS device in TN4 is based on a larger micro mirror from Sercalo which is used in the Tuneable Filter product. Based on this experience the predicted specifications in terms of max. tilt angle and resonance frequency, could be realized with only one manufacturing run.

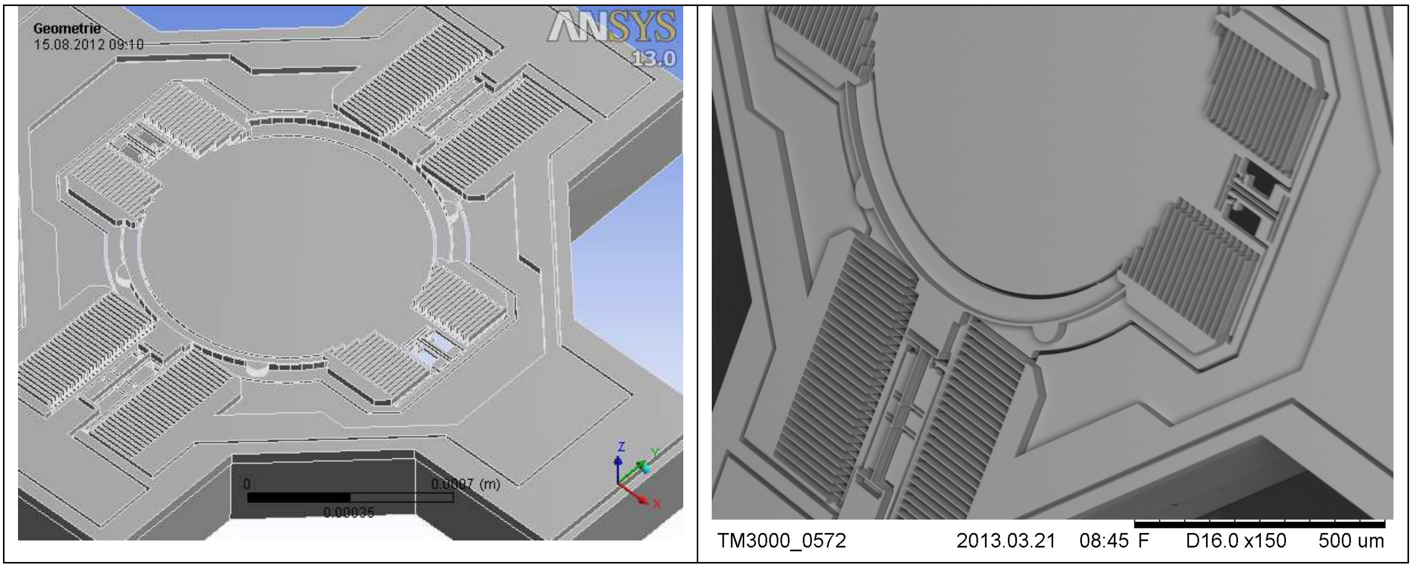

Figure 1: Left, the geometry of the MEMS simulated in TN4. On the right side the SEM picture of the fabricated MEMS mirror.

To validate the robustness against thermal induced stress on the mirror surface, a measurement of the radius of curvature at different temperatures was done with an white light interferometer (WYKO). The results are summarized in Table 1.

Table 1: Results of the ROC measurement

	Measurement @ +25°C		Measurement @ +80°C	
	ROC X Profile [m]	ROC Y Profile [m]	ROC X Profile [m]	ROC Y Profile [m]
Measurement	1.8	2.8	22.0	11.0
Requirement	0.8	0.8	0.8	0.8

All other specifications and results can be found in the PCM in the end of this document.

Figure 2 depicts the compact MEMS scanner with a volume of ~1.2 cm^3, which is only 1/10 of the required specification in the SOW of <12cm^3. This package consists of a standard TO8 socket, the electrostatic MEMS mirror with D=1mm and a lid with integrated fiber collimator and glass window.

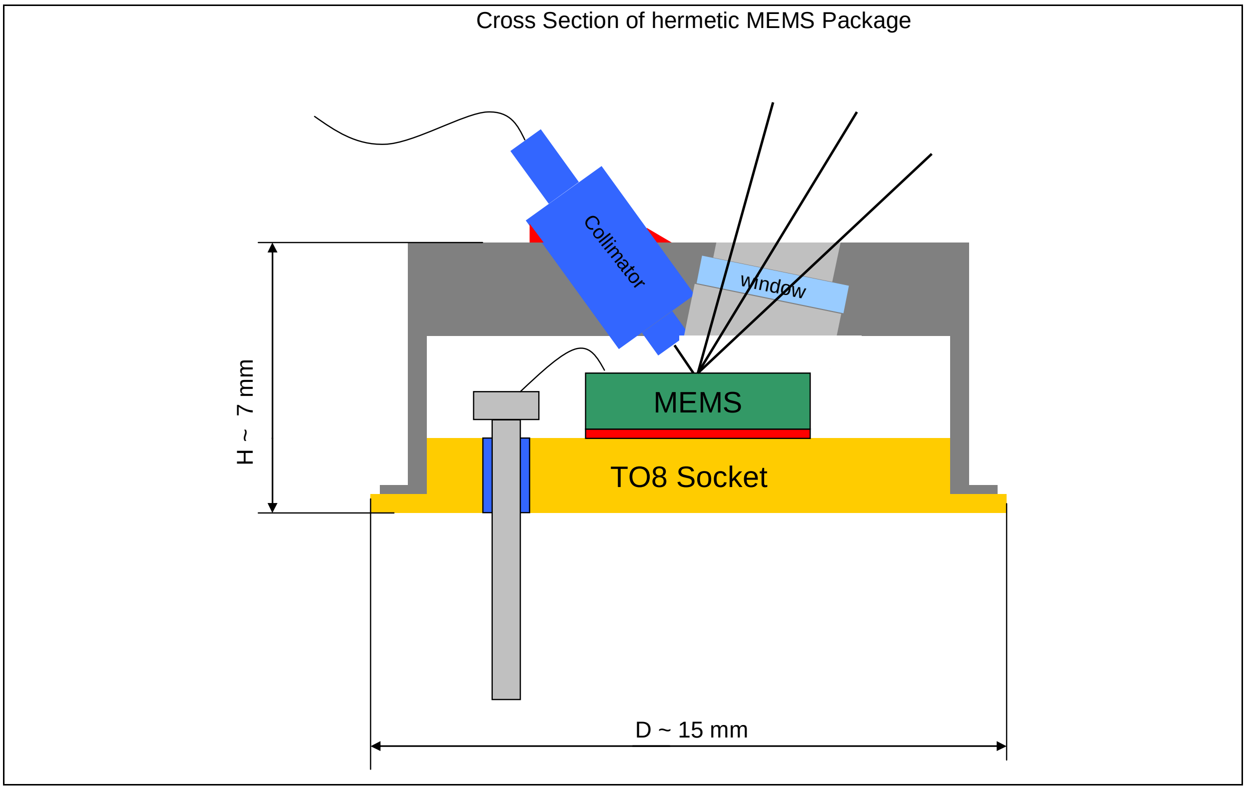

Figure 2: Cross section with main dimensions of the MEMS scanner.

Figure 3: Twelve MEMS Units ready to enter the environmental test program.

Figure 4: Open scanner housing.

In the end of the manufacturing and assembly part of the project, two fully assembled Scanner Units and 21 MEMS packages (mixed oil and non damping versions) entered the environmental testing.

4 ELECTRONICS

The MLBS contains a MEMS micro-mirror which is controlled by actuation electronics. In addition, this electronics provides sensing circuits for the mirror position. The implementation of the digital part of this electronics evolved during the development and is referred to as SAU-2 (Sensing and Actuation Unit – version 2).

The MEMS micro-mirror is controlled in horizontal and vertical axes using the electrostatic actuation principle. This means generating forces by applying actuation voltages on mirror moving combs. These forces are then balanced by the etched comb springs resulting in a mirror tilt angle dependent on the applied voltage. The architecture of the mirror control electronics is shown in *Figure 5*.

The mirror tilt angle is a non-linear function versus the applied actuation voltage and therefore, to make the linear output, the proper voltage levels shall be stored in a look-up table of the digital control logic. Since positive and negative voltages generate the same force (attraction) the negative voltages cannot be used to reverse the mirror angle. To change the direction of the tilt the voltage shall be applied to the other side of the mirror comb, thus requiring two actuation outputs per mirror axis. Therefore, in total four actuation outputs are required for the bidirectional mirror angle control in two axes.

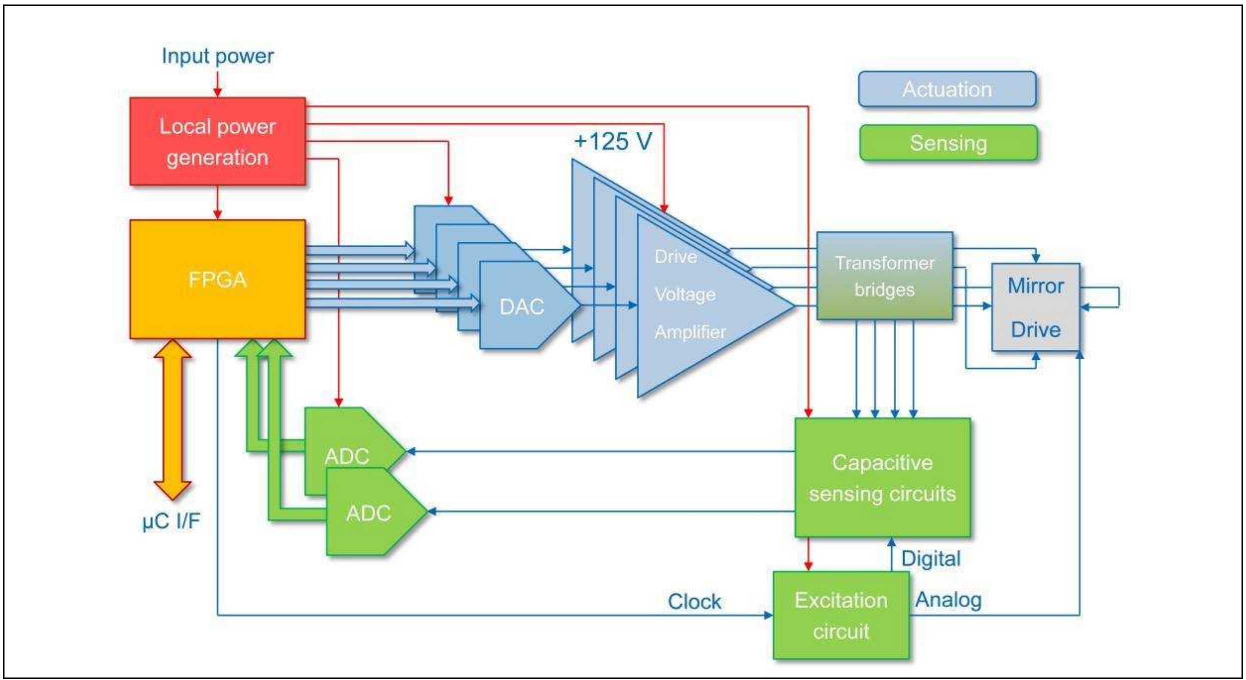

Figure 5 : Electronics block diagram (SAU-2)

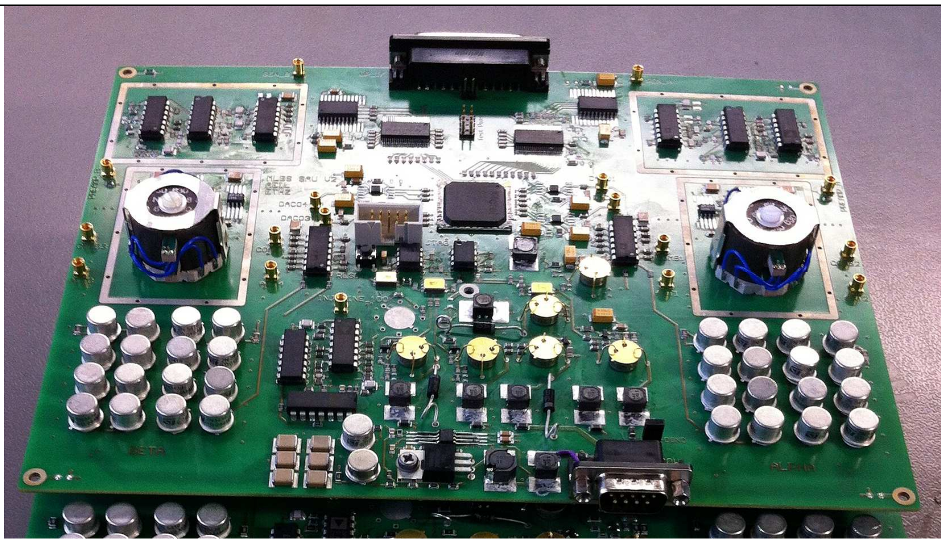

Figure 6 : Realized SAU-2 electronics

5 ENVIRONMENTAL TESTS

The environmental test campaign was made in two parts. In 2012 a pre-test campaign was made with early prototypes of the micro mirrors. The aim of the pre-test was to prepare and verify the test setups of the MLBS MEMS devices as well as to obtain first results of the tolerance of the MLBS micro mirrors to environmental hazards. The pre-test campaign included mechanical vibration and shock tests, thermal cycling and ^{60}Co γ-ray irradiation. The results obtained were used in the latter phases of the development, manufacturing and testing of the MLBS devices.

The final test campaign performed in 2013 aimed at demonstrating the ability of the MLBS micro mirror devices to withstand the environmental conditions defined in the SoW. In the final environmental tests, all tests were performed in succession. The sequence of the tests has been defined in TN 2 “Performance verification and test plan” and is represented in Figure 7. The environmental testing related to the MLBS was performed at different institutions (Table 2), directly followed by the Quality Control Section. Most tests were performed at CSEM, Sercalo or ESA-ESTEC.

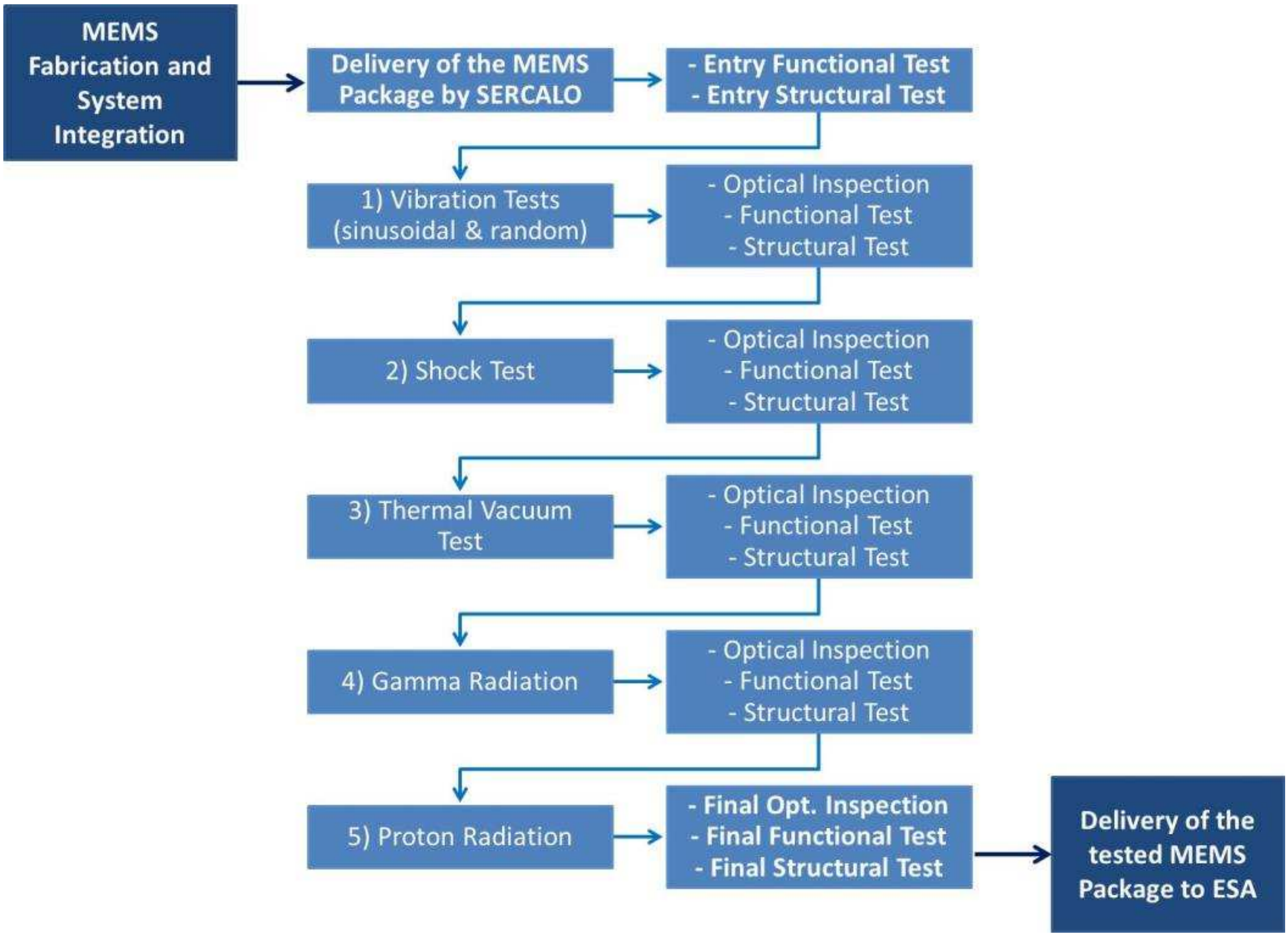

Figure 7: Environmental test matrix

Table 2 : Test Table for the Environmental Testing.

Environmental Test	**Tests to perform**	**Test Location**
Mechanical shock and vibration	- Sinusoidal - Random vibration	ESA-ESTEC, NL (TIRAvib TV50350 shaker table. Provides random and sinusoidal vibrations of up to 60g.)
	- Shock (0 to peak amplitude: 3000g)	ESA-ESTEC, NL (L.A,B. SD-10: shock tester available. Shocks of up to 5000g.)
Thermal Vacuum	Temperature range: -130°C <--> +20° (8 cycles in thermal cycling)	ESA-ESTEC, NL (Vacuum thermal cycling chamber by Vacuum Specials. Temperature range +/-140°C, vacuum level ~10^{-5}mbar.)

Radiation	- Gamma radiation: Total dose: 20 krad	a) ESA-ESTEC, NL ESTEC's Cobalt-60 facility
	- Proton radiation: 20 krad	a) Proton Irradiation Facility (PIF) at the Paul-Scherrer Institute (PSI), Switzerland

5.1 RANDOWM VIBRATION TEST

The vibration level requirements depended on the total mass of the MLBS (ECSS-E-10-03A, p. 56). For the MEMS components a device mass of 0 g was assumed and consequently the random vibration qualification level was 37.7 g_{rms} (52.4 $g_{peak\text{-}to\text{-}peak}$). The test duration was 2.5 min/axis. For the scanning units, which weighed 0.2 kg, the test level was 34 g_{rms} (48.1 $g_{peak\text{-}to\text{-}peak}$). The required acceleration spectral density (ASD) of the random vibration test is shows in Figure 8 and an example of an experimentally measured ASD spectrum is presented in Figure 9.

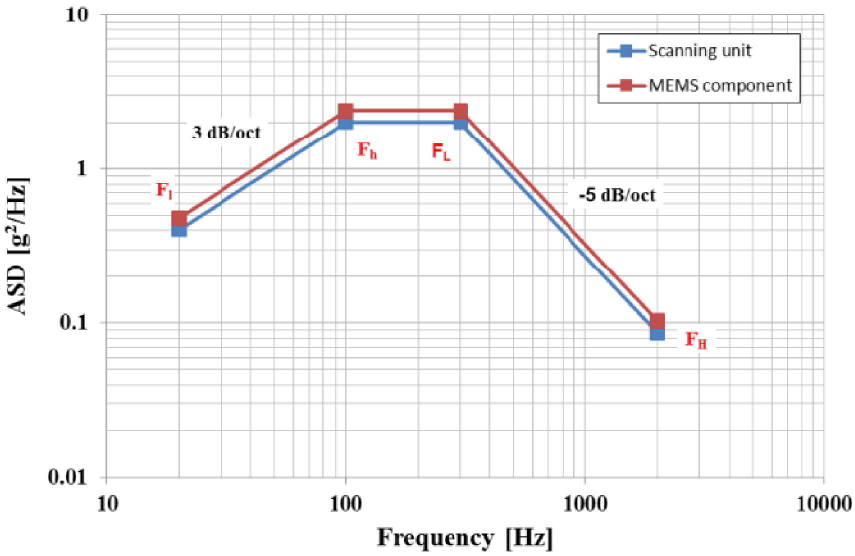

Figure 8 – Acceleration spectral density (ASD) in the bandwidth of random vibration tests.

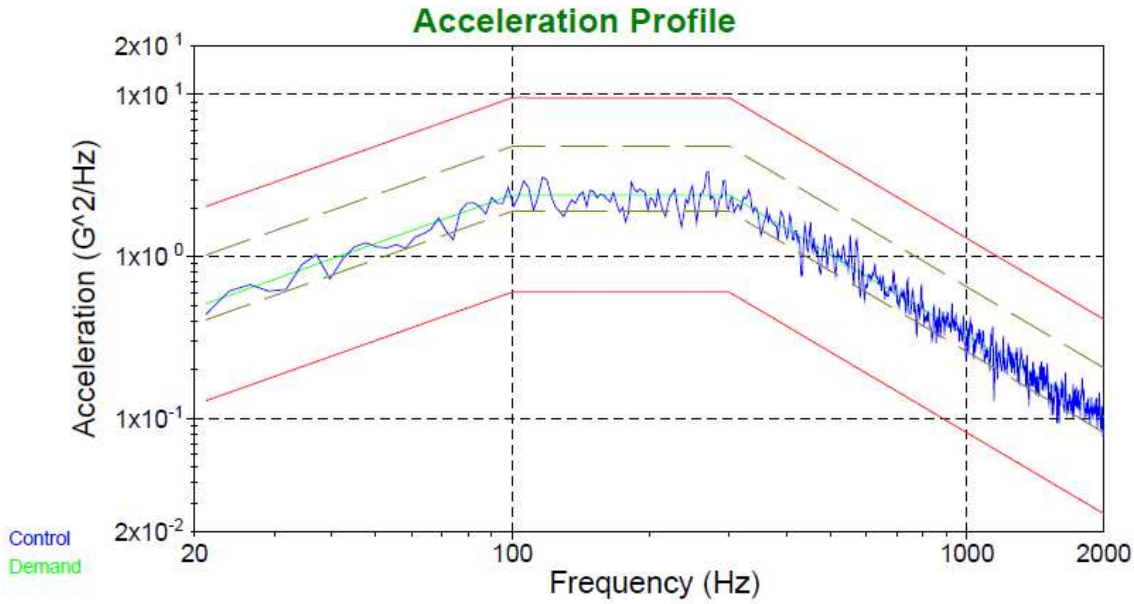

Figure 9 – Experimental acceleration spectral density of a MEMS component.

5.2 SHOCK TESTS

The shock tests were conducted at ESA-ESTEC (see Table 2), according to the test plan (Technical Note n°2 Performance verification and Test Plan), using a L.A.B. SD-10 free fall shock tester system. Three Shocks were imposed along both directions of three orthogonal axes, adding up to 18 shocks. At 3000g most of the devices passed the test without signs of degradation.
The qualification levels for the shock amplitude and shock duration were a peak acceleration of 3000g and pulse duration of 0.3ms. The pulse duration has been selected based on the Military standard MIL-STD-883H (Method 2002.5)

5.3 THERMAL VACUUM TEST

The conditions encountered in space include large variations in temperature and high vacuum. Thermal vacuum tests simulate these conditions and allow demonstrating the stability and correct functioning of the devices subjected to in-orbit thermal conditions. The thermal vacuum tests protocol was based on ECSS-E-10-03A, section 5.1.15 and section 5.1.16 and was described in the test plan (Technical Note n° 2 Performance verification and Test Plan).

Figure 10 shows the devices mounted inside the TVC chamber. The specimens were placed on the base plate, which is a hollow box through which the liquid nitrogen flows during the experiment. Aluminium tape was used to improve the thermal contact with the base plate. The temperature was measured at various points of the base plate and on the samples.
Figure 11 shows the temperature profile during the thermal vacuum cycling test. The thermocouple “Channel 3” was placed near the base of the T08 sockets. Another

thermocouple (Channel 4) was placed on the sidewall of one of the scanning units (P1). Two thermocouples were placed onto the base plate (Channel 5 and Channel 6), one of which, however, had a loose contact and therefore displayed an unusable signal. The “Base plate” signal corresponds to a thermocouple which was permanently integrated into the base plate.
The behaviour of the chamber was tested without the specimens but with metal plates with the same weight (7mm thick aluminum), simulating the thermal masses. At temperatures below -90°C the temperature of the metal plates started to deviate from the base plate temperature, and cooled more slowly. In order to compensate for the slower cooling of the devices the following adjustments were made on the test parameters when testing the MLBS devices:

- the target temperature was set to -145 °C, instead of -130 °C.
- the dwell time was increased from 2h to 2.5 h.
- the cooling rate was set to 10 K/min instead of 20 K/min.

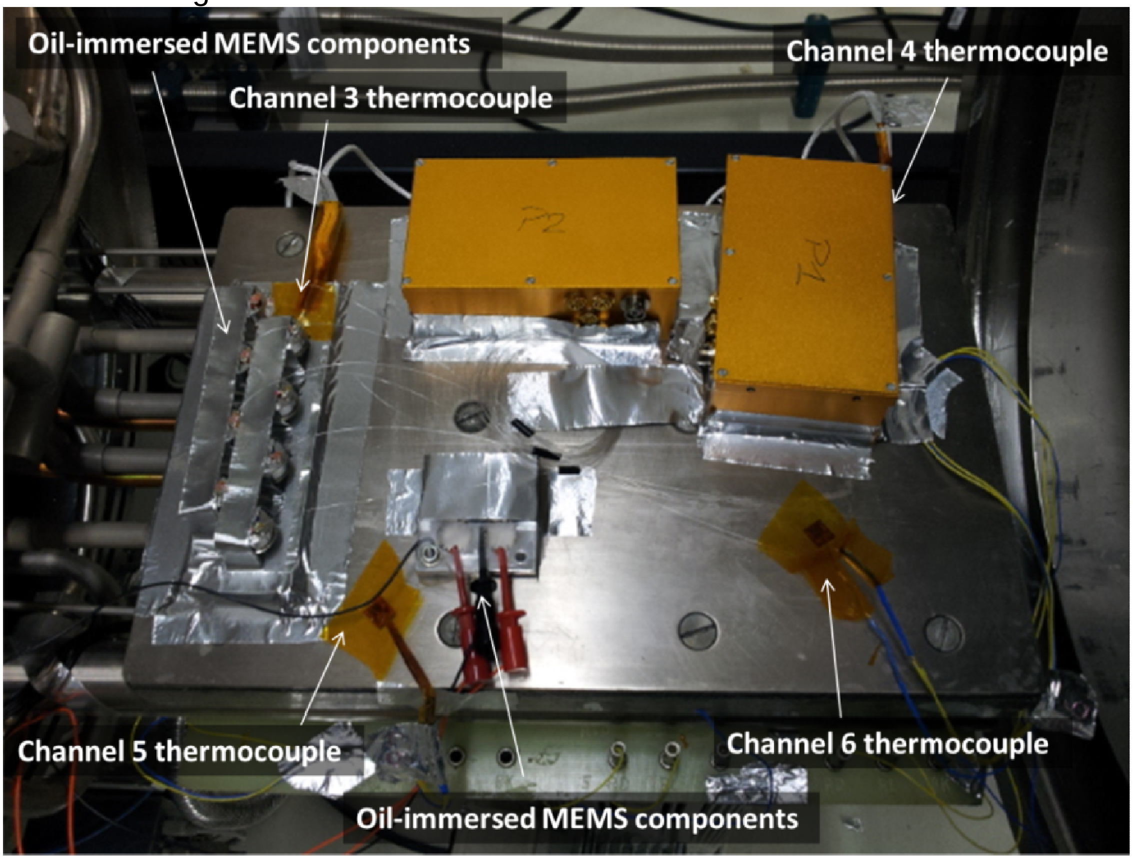

Figure 10 – Sample installation for thermal vacuum cycling test.

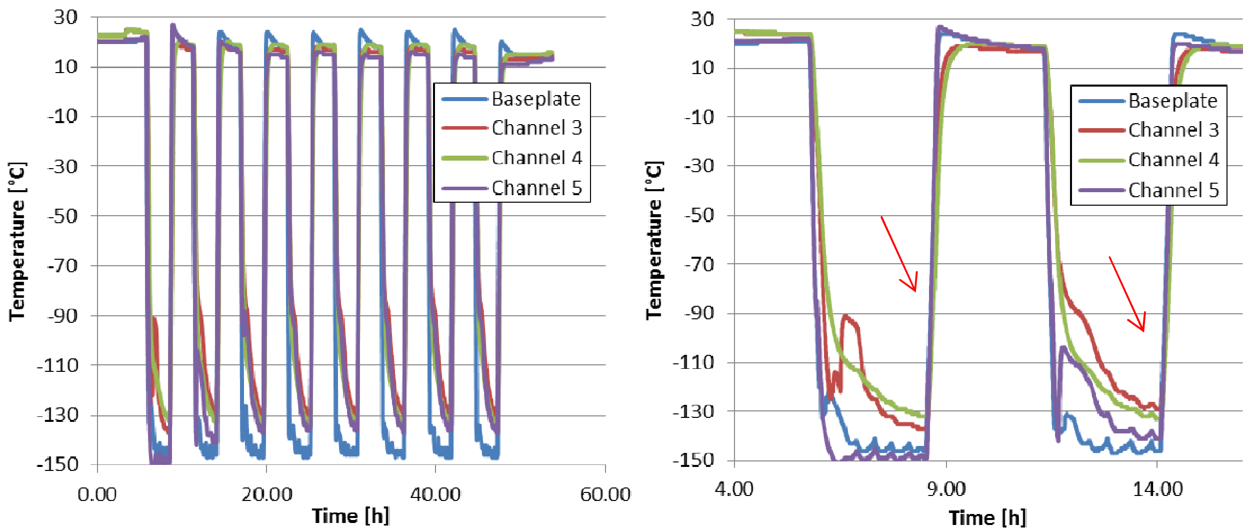

Figure 11 – Temperature profile of the TVC test. The left graph shows the entire test with totally eight cycles. The right graph shows only the first two cycles. The thermocouple of channel 3 was placed near the oil-immersed MEMS components.

5.4 ^{60}Co Γ-RAY IRRADIATION TESTS

Total dose radiation tests using gamma-rays aim at evaluating the susceptibility of the MEMS devices to ionizing radiation. The ^{60}Co ã-ray irradiation protocol was based on ESCC Basic Specification No. 22900 and was described in the Technical Note n° 2 “Performance verification and Test Plan”. The ^{60}Co ã-ray irradiation tests were conducted at the ESA-ESTEC Co-60 facility in Noordwijk, The Netherlands.

Results from pre-tests (May-June 2012): The total ionizing dose (TID) test setup has been prepared and verified during the pre-tests of MLBS MEMS devices. During the pre-tests all device pins were grounded. They were irradiated at a dose rate of 5.4 rad(Si)/h. The total dose was increased step-wise and functionality tests were made at each level (Figure 12). After the irradiation the devices were annealed at room temperature during four weeks. During the whole pre-test campaign no failure of an axis has occurred and the basic functional tests have not revealed any deterioration of the performance of the micro mirrors.

Dose Level	Total Dose [krad]	Day
1	3	0
2	12	1
3	36	2
4	51	3
5	99	4

Figure 12 – Radiation parameters in the TID pre-tests.

Due to the large thickness of the top-side of the T08 cap which was 2.3 mm, the specimens were placed horizontally. In this way only 0.175 mm of metal (INOX 1.4301) and a 5 millimeters of oil shielded the silicon MEMS components.

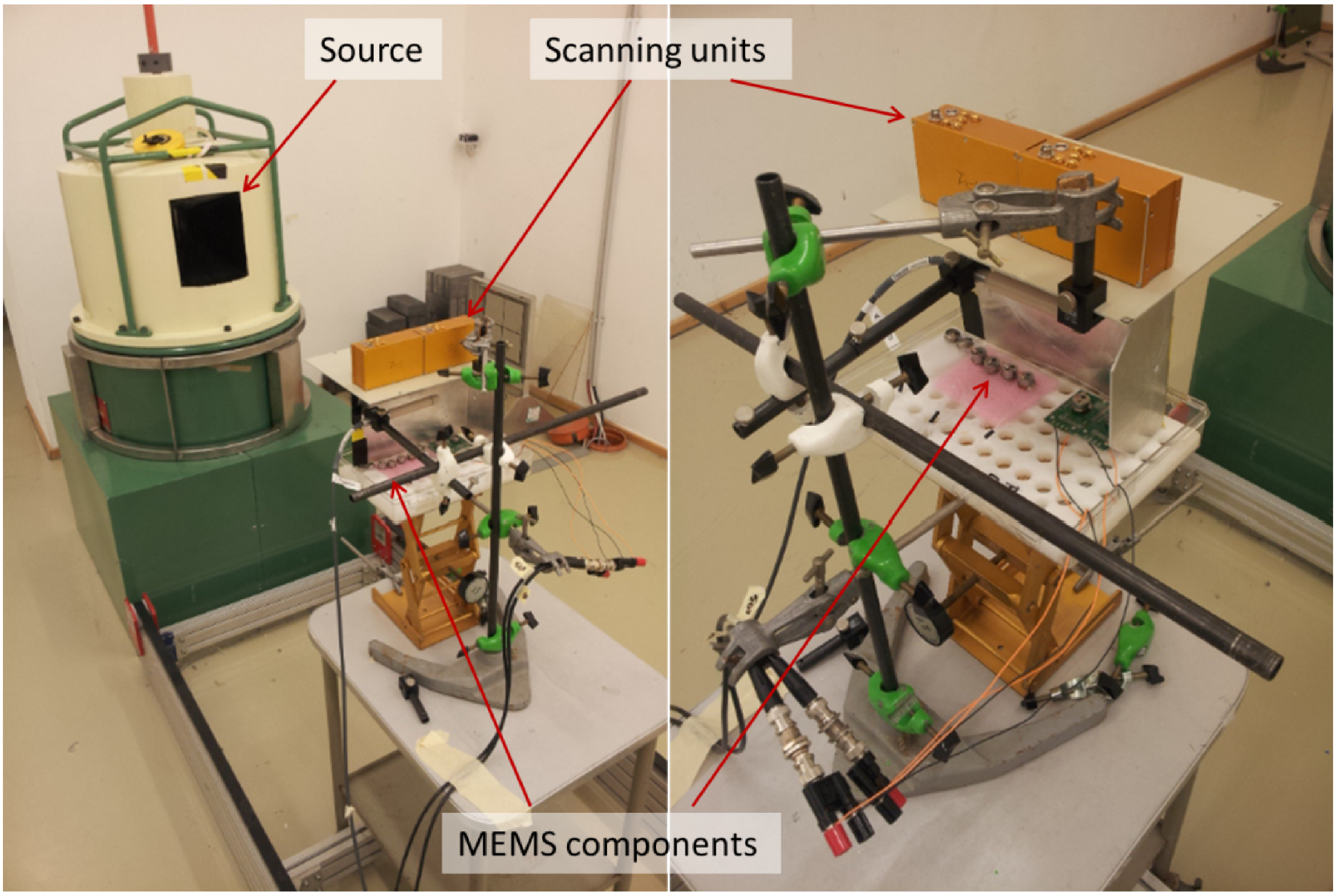

Figure 13 – Sample setup for the Co-60 gamma-ray irradiation.

After the end of the irradiation, the functional characterization was immediately started. All devices were functionally characterized within 2h after the end of the irradiation.

5.5 PROTON IRRADIATION TESTS

Proton irradiation tests aim at evaluating the susceptibility of the MEMS devices to ionizing damage and displacement damage. The proton irradiation protocol was described in the Technical Note n° 2 "Performance verification and Test Plan". The proton irradiation tests were conducted at the Proton Irradiation Facility (PIF) at the Paul-Scherrer Institute in Villigen, Switzerland.

The protons must have sufficient energy to fully penetrate the device package. Using SRIM-08 the proton irradiation of the packaged devices was simulated. In these simulations the sample structure consisted of the following stack:

- 0.175 mm Stainless Steel

- 5 mm oil (The stoichiometric ratio between the element Si, O, C and H was 1:1:2:6)
- 2mm silicon

The trajectories of the proton in the package are shown in the right graph of Figure 15 for the selected proton energy of 50 MeV. This proton energy ensures full penetration of the protons into the device and over 99.9 percent of ions fully penetrated the simulated layers.

The selected proton fluence of $1.26 * 10^{11}$ p cm^{-2} corresponds to 20 krad at the surface of irradiated silicon without any shielding layers. At these conditions the stopping power (i.e. the energy deposited per unit path length is 0.23 eV/Å.

In the real packages the silicon MEMS components were shielded by the layers mentioned above. The effect of these layers was to reduce the energy of the protons on their trajectory towards the silicon micro mirror due to the energy loss during the passage through the package. Because the stopping power is inversely related to the ion energy, an energy loss results in higher radiation damage. Therefore, the energy loss in the silicon was higher in the shielded device than in directly irradiated silicon by approximately 10-30% and the effectively absorbed dose in the MLBS micro mirror was increased correspondingly.

irradiation.

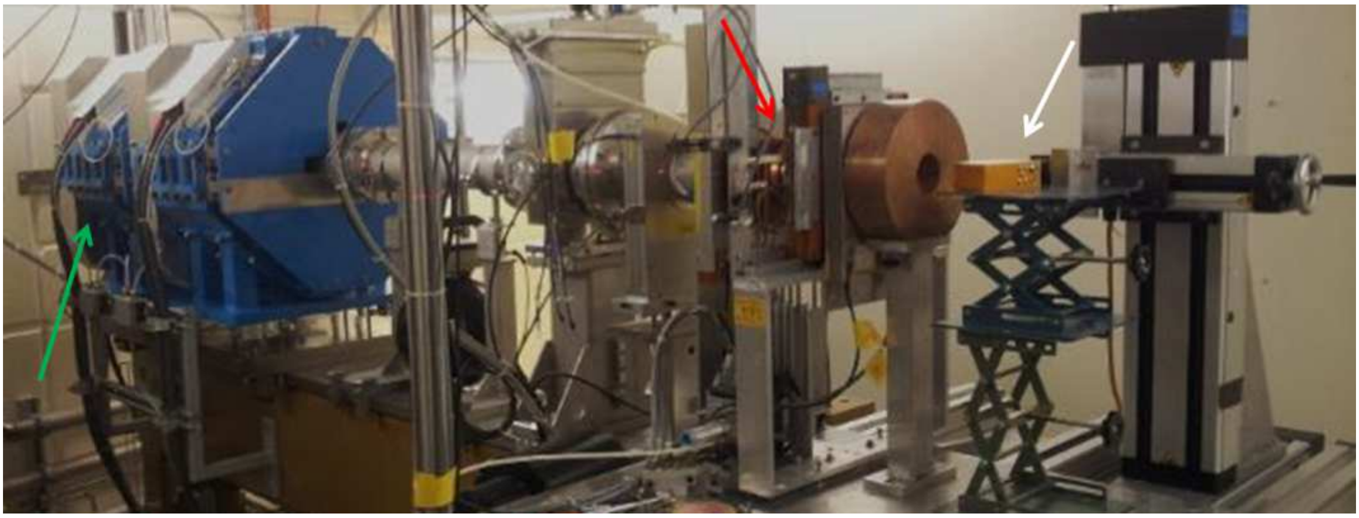

Figure 14 – Image of the proton irradiation beam chamber. The proton beam enters through the wall at the left side (indicated by the green arrow) and is shaped i.e. by the blue magnets. The proton energy is adjusted by degraders (metallic plates which are inserted or retracted from the beam path, red arrow) before the beam hits the sample (white arrow).

Proton irradiation test results

All irradiated devices passed the test without any signs of radiation-induced damage (floating, biased and unbiased devices). For the oil-filled devices one axis recovered during the test, therefore the fraction of surviving axes is larger than 1 (**Fehler! Verweisquelle konnte nicht gefunden werden.**, page **Fehler! Textmarke nicht definiert.**). However, this was presumably related to a reversible blocking of the mirror and was independent from the irradiation test.

In addition to these tests, four MLBS micromirrors from the pre-test campaign (T05) have been irradiated in 20 krad steps up to 60 krad. No changes in the functionality or leak-currents were observed in these devices.

Due to elevated radioactivity the devices were not directly released by the radiation facility. The activity of the samples was monitored until safe levels were reached, which was the case three weeks after the irradiation. After this, the specimens were returned to Sercalo for further characterization of the functional performance.

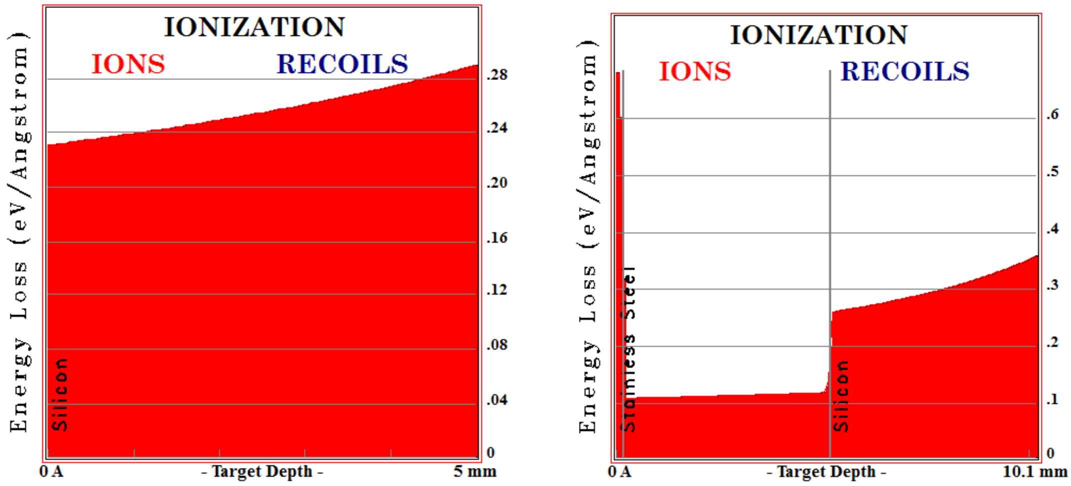

Figure 15 – Energy loss of 50 MeV protons when striking silicon (left graph) and the TO8 MLBS package (right graph). Note that the y-scales are not the same for the two graphs.

6 ACHIEVED PERFORMANCE

In the following tables, all requirements and the achieved performances are summarized.

Table 3: Functional Requirements

Requirement object	Required specification	Compliant	Achieved Performance	Comment
Functional				
Func4 Laser Beam Divergence	0.5° horizontal 0.5° vertical	C	0.15°	
Func5 Laser Wavelength	1550nm	C	1550nm	For DEMO Red Laser Light
Func6 Mirror Dimension	>= 1mmx0.7mm	C	D=1mm	
Func7 Mass of MLBS	<=60g	NC	190g including connectors and housing	Only the scanner itself 7,9g
Func8 Volume SU	<=12 cm^3	NC	216cm^3 including connectors Without connector, 1.2cm^3	
Func9 Volume EU	No spec. in SOW	C	240x190x40mm	

Table 4: Performance Requirements

Requirement object	Required specification	Compliant	Achieved Performance	Comments
Performance				
Perf2 Field of Regard	22° horizontal 22° vertical	C	24.3° ± 0.4 horizontal 24.7° ± 0.4 vertical	With 80V actuation Voltage
Perf3 Scene coverage	>90%	C	>90% when using 0.5° divergence and 100x100 points	Combination of Spot diameter and scan point list
Perf4 Scan time ts for the whole FoR	FoR/α^2*10µs<ts<1s	C	1s	Design and Lookup table
Perf5 Mirror scan speed variation	<5%	C	As discussed with ESA, this requirement is only applicable in the centre of the scan scene	Design
Perf6 Life-time	>2 years operational >4 years non operational	C	Hermetic TO8 Package	Design
Perf7 Mirror flatness	<λ/10	C	0.155µm over R=500µm mirror --> ROC>0.806m Measured ROC>1.8m	Wyko Measurement
Perf8 Maximum wavefront error of the scanner optics	<λ/3	C	< λ/4	Design
Perf9 Resonance frequency	>160 Hz	C	>300 Hz	Measured
Perf10 Peak power consumption	<=5W	C	3,495 W	Measured
Perf11 Average power consumption standby	<=1W	C	0.717 W	Measured
Perf12 Optical pointing stability	@ any angle within FoR, during 10seconds: ± 4mrad threshold ± 0.2mrad (goal)	C	<0.6 mrad +/- 0.2	Our mirror is not driven in resonance → static pointing possible. 12bit resolution of the electronics = 0.023mrad. No charging effects seen in pre tests--> no drift source.

Table 5: Functional Requirements (continuation)

Perf13 Angular position knowledge accuracy of the optical beam	±0.025°	PC	Alpha 0.4°, Beta 0.03°	
Perf14 Cross coupling between scan angle axis	Shall be <0.25° for entire FoR	C	Independent axes due to design of vertical comb drive	

Table 6: Interface Requirements

Requirement object	Required specification	Compliant	Achieved Performance	Comments
Interface				
Intf1 Laser beam input	FC/APC or FC/PC	C	FC/PC	
Intf2 Power supply	3V, 5V, 15V, 28V	PC	Required voltages are +3.3V, +/-15V, +/-7.5V, 28V	Design
Driver Interface	-	C	RS 232	Commands and protocol definition in the supplied manual

Table 7: Environmental Requirements

Requirement object	Required specification	Compliant	Achieved Performance	Comments
Environmental				
Env1 Temp operational SU	-70°C to +20°C	C	-70°C to +20°C	
Env2 Non operational Temp. SU	-130°C to +70°C	C	-130°C to +70°C	ROC of mirror before and after -130°C treatment.
Env3 Temp operational EU	-20°C to +40°C	C	-20°C to +40°C	
Env4 Non operational Temp. EU	-20°C to +70°C	C	-20°C to +70°C	
Env5 Pressure	1mbar to 1.2bar	C	Hermetic package	
Mechanical Vibration	Sinusodial 37,7 g	C	37,7g	
Mechanical Vibration	Random Noise 37,7g	C	37,7g_{rms}	The random vibration qualification level was 37.7 g_{rms} (52.4 $g_{peak\text{-}to\text{-}peak}$). The test duration was 2.5 min/axis. For the scanning units, which weighed 0.2 kg, the test level was 34 g_{rms} (48.1 $g_{peak\text{-}to\text{-}peak}$).

Table 8: Environmental Requirements (continuation)

Requirement object	Required specification	Compliant	Achieved Performance	Comments
Mechanical Shock	3000g	C	3000g	The qualification levels for the shock amplitude and shock duration were a peak acceleration of 3000g and pulse duration of 0.3ms.
Thermal Vacuum Test	8 cylces -130°C to +20°C in 10^{-5} mbar	C	-145°C to +20°C	10K/min. dwell time 2.5h
Gamma Radiation Co^{60}	Total Dose 100krad	C	100krad	A dose rate of 5.4 rad(Si)/h
Proton Radiation	target fluence of 1.26 * 10^{11} p cm^{-2} total dose 60 krad	C	1.26 * 10^{11} p cm^{-2} total dose 60 krad	2 weeks quarantined due radioactivity

Two deliverables passed successfully all requirements and we fulfilled the specifications given in the Statement of Work.

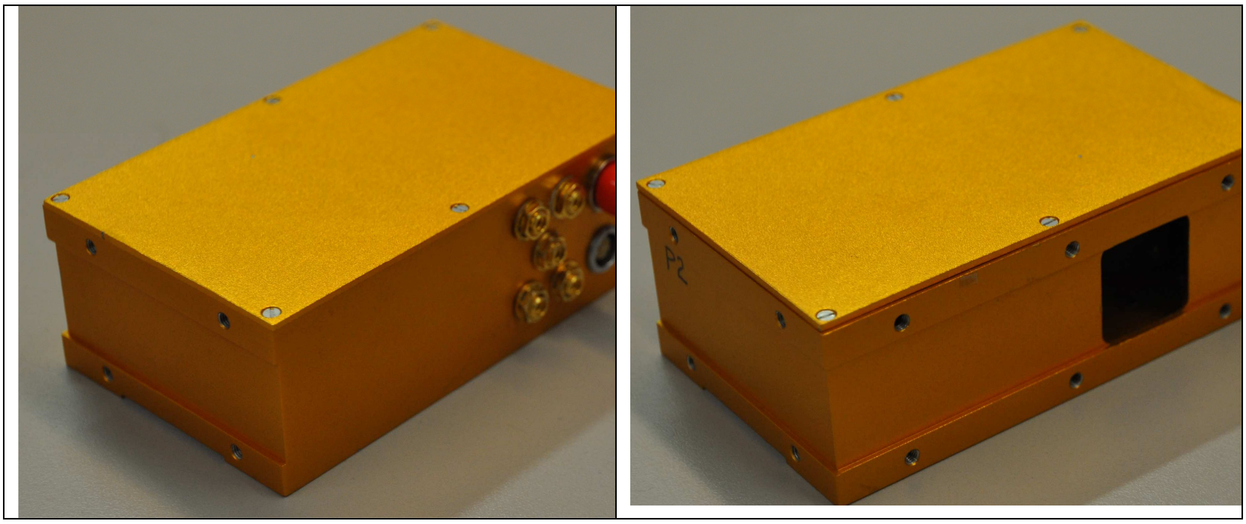

Figure 16: Front and backside of one Scanner Unit closed. For interconnect a FC/PC plug and five MMCX connectors for driving and sensing are available. The Lemo connector is for optional heating.

7 CONCLUSION AND PERSPECTIVES

Since the electrostatic MEMS devices are intrinsically non-linear, the optical scanning path is generated from a lookup table that contains a list of the passage points. Due to the assembly tolerances, the lookup table is unique for each scanner device and a complex procedure is required in order to characterize it and calculate the list of points. This approach can not completely compensate the non-linear behavior of the system and a residual overshoot can be measured.
Based on the experience gathered during this project and we can give the following recommendations:

- Electrostatic driven MEMS mirror devices can be used up till max. 1mm mirror diameter for static pointing and scanning option for the given performance of 22° FoR and 1s scan time. Vertical comb drives are limited by the thickness of the Silicon layers of the wafer. When the comb drives are placed more fare from the tilting axis, the delta in height increases and so the possible tilt angle decreases. If a bigger mirror (e.g. 15mm) is required, magnetic driven mirror can be used.
- An additional advantage of a magnetic driven mirror is the linear relation ship between driving current and tilt angle. As mentioned before, a complex procedure is required to drive the mirror. When the relation ship is linear, a simple formula can be used as base for driving.
- Liquid damping increases the complexity of the whole system (additional heating, thermal compensation structures) and should be only implemented if electronic and/or software damping solutions fails.

The potential of future developments of MEMS based scanners is not yet fully discovered. With a clever design, it can bring benefits in terms of compactness, cost reduction, and functionality.